Mem. S.A.It. Vol. 78, 48

Memorie della

Contrast inversion in the 557.6 nm line detected with differential speckle interferometry

C. Grec[1], C. Aime[1], M. Faurobert[1], G. Ricort[1], and F. Paletou[2]

[1] Université de Nice Sophia Antipolis, Laboratoire Universitaire d'Astrophysique de Nice (UMR 6525), Parc Valrose, 06108 Nice cedex 2, France
[2] Université Paul Sabatier, Toulouse 3, Observatoire Midi-Pyrénées, Laboratoire d'Astrophysique (CNRS/UMR 5572),
14 avenue Edouard Belin, F-31400 Toulouse, France

Abstract. We report on some aspects of the use of a Differential speckle interferometry technique on the Sun. The method consists in cross-correlating images of the granulation taken in the line absorption and in the continuum, outside the solar disk center. Due to a perspective effect, the difference in depth between different photospheric levels results in a difference in position along the spectrograph slit. Observations were done in 2002, 2005 and 2006, at the telescope THEMIS in the 557.6 nm iron line. As expected from the perspective effect, we obtain opposite results at opposite latitudes on the Sun disk. Surprisingly, the displacements measured in the blue and the red wings of the line have opposite signs. This may be the result of unresolved Doppler shifts produced by horizontal granular velocity fields. We also detect an anti-correlation peak in the core of strong lines, that is the signature of a contrast inversion.

Key words. line: profile – Sun: granulation – techniques: differential speckle interferometry

1. Introduction

Classically in solar physics, the vertical structure of the photosphere is studied with spectroscopic methods. At this Solar Dynamics & THEMIS users meeting, we proposed an alternative that consists in using a Differential speckle interferometry (DSI) high-resolution technique. DSI is not seeing-limited (Beckers & Hege 1982; Aime et al. 1984, 1986), and allows shifts smaller than the telescope Airy disk to be measured (on the order of 0.01"). Thus we can very precisely determine the line formation depth and the depth-range on which photospheric structures remain similar to themselves, with no need to calibrate the atmosphere's modulation transfer function. These informations can be obtained directly from the phase of the cross-spectrum. DSI capabilities in our particular case are extensively described in Grec et al. (2007) (in press, named as Paper [1] in the following).

2. Solar DSI principle

Our experiment is based on the fact that two overlapping structures in the photosphere, observed outside the disc center, will appear hor-

Send offprint requests to: catherine.grec@unice.fr

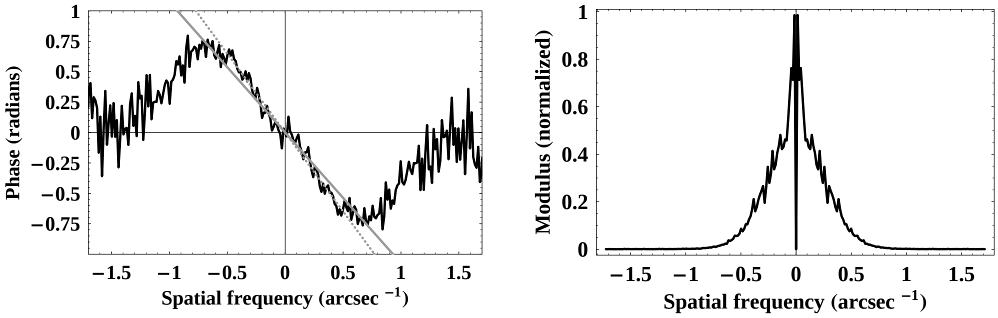

Fig. 1. Determination of the displacement ε between line and continuum structures: phase (right) and log-scale modulus (left) of the cross-spectrum, calculated between the continuum and the blue wing of the 557.6 nm line. The phase is linear in the spatial frequency domain corresponding to a significative power of the cross-spectrum modulus (for $u \in [0.2; 0.78]$ arsec^{-1}).

izontally displaced when one is compared to the other. Orienting the x-axis in the South-North direction, we expect the displacement ε to be positive for north latitudes, negative for south latitudes and null at disk center. ε linearly depends on the difference of depth between the structures and on the sinus of the angle between the position and the view-sight. We measure the 1D brightness intensity along the slit, denoted by $I_\lambda(x)$. An observation $I_W(x)$ made in the wing of a line corresponds to a higher formation level in the photosphere than the image $I_C(x)$ taken in the continuum of the spectrum. Outside the disk center $I_W(x)$ appears shifted towards the limb in comparison to $I_C(x)$. If the structures that exist at different photospheric levels are similar, we can write:

$$I_W(x) \sim I_C(x-\varepsilon), \tag{1}$$

After the Fourier transform, we get:

$$\widehat{I_W}(u) \sim \widehat{I_C}(u)\exp(2i\pi u\varepsilon). \tag{2}$$

We use a series of spectrograms to estimate the cross-spectrum $\widehat{Q_{CW}}$ between $I_C(x)$ and $I_W(x)$:

$$\begin{aligned} \widehat{Q_{CW}}(u) &= <\widehat{I_C}(u)\widehat{I^*_W}(u)> \\ &\sim <|\widehat{I_C}(u)|^2> e^{-2i\pi\varepsilon u}, \end{aligned} \tag{3}$$

where $\widehat{I^*_W}(u)$ represents the conjugate Fourier transform of $I_W(x)$, and the brackets refer to the ensemble average. In this case, the amplitude of the cross-spectrum $<|\widehat{I_C}(u)|^2>$ is identical to the power spectrum of the granulation, attenuated by the instrument/atmosphere modulation transfer function (Aime 1974). We show in Fig.1 an example of cross-spectrum (phase and modulus) allowing to derive ε from the slope of the phase. The similarity of the images in the line and in the continuum is essential for these measurements, which is not the case near the center of strong absorption lines formed over large depths in the photosphere. These aspects are more developed in Paper [1].

3. A first run in 2002, on THEMIS

Our 2002 data material consists in high-spectral resolution spectrograms, recorded at the THEMIS[1] telescope in September 2002 with the MTR mode. We observe the solar spectrum in a 5Å region around the 557.6 nm non magnetic iron line, with a wavelength sampling of 12.5 mÅ/px. The spectrograph slit is 70″ long and its direction is set perpendicular to the solar edge, along the North-South axis. The pixel sampling is of 0.29″. The observations are done on a quiet Sun, at opposite latitudes for $\mu = 0.86$ and $\mu = 0.66$. To improve

[1] THEMIS is operated on the Island of Tenerife by CNRS-CNR in the Spanish Observatorio del Teide of the Instituto de Astrofisica de Canarias.

the statistic on the granulation power spectrum, we scan a region of about $70'' \times 70''$.

The exposure time is 300 ms, which does not allow the atmospheric turbulence to be frozen. We only select the spectrograms recorded when the r_0 parameter has a quite high value. The highest spatial scale detectable in the power spectrum of the granulation was $0.78''$.

4. Improvements during 2006 THEMIS observations

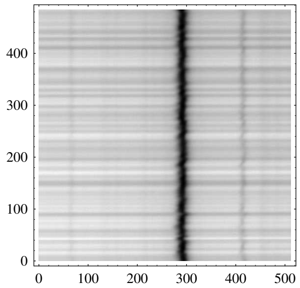

Fig. 2. Spectrogram recorded on Sept. 8^{th}, 2006, with the new Ixon camera (512×512 pixels), at THEMIS.

For technical reasons, the observations made in 2005 were of too bad quality to be processed. A new observation was made in September 2006, using a new CCD Ixon camera, and the data are still being treated. The spatial pixel size is of 0.155" and the first results are given here. The observing procedure remains similar to that of 2002 with a few improvements. The slit is of 0.25 large, the wavelength sampling is of 7.56 mÅ/px, and we added three positions ($\mu \in \{0.66, 0.86, 0.97, 1\}$). The new camera allows us to take images with a time integration more adapted to the DSI technique (on the order of 10ms). A 50ms value seems to be a good compromise between the atmospheric freezing and a good signal-to-noise ratio of the absorption profiles in strong lines. This is necessary because, before calculating the cross-spectra, we need to correct the spectrograms from the line shifts due to the Doppler effect of granular velocity fields (see Fig.2).

5. From the cross-spectrum phase to the line formation depth

We used different simplified procedures to estimate the slope of the cross-spectrum phase. The more robust one consists in determining it with a linear fitting that takes into account a limited range of frequencies. In this case, when noise begins dominating signal, the highest signal frequencies do not contribute to the slope determination. We present here some results obtained from the 2002 observations.

5.1. Results: phase behaviors

As expected from the perspective effect, we obtain displacements with opposite directions for the observations made at the North and South latitudes. However, we found an unexpected effect: whatever the spectral line or the position on the Sun disk, the slopes of phase have opposite signs in the blue and red wings of the line (see an example in Fig.3).

5.2. Interpretation

In Fig.4, we show the shifts derived from the phases measured for the North-South positions at $\mu = 0.86$ in the 557.6 nm spectral domain. Both wings of a line are formed at higher altitudes than the continuum. That is why the change in sign of the displacement from the red to the blue wing cannot be due to a perspective effect.

However, we may interpret this as the effect of uncorrected granular velocity fields. Let us consider a granule that rises and expands from the bottom of the photosphere to the most external layers. The monochromatic images seen in the red and the blue wings of an absorption line are due to the contributions of different regions of the granule. The granule material moving horizontally towards the Sun pole is moving away from the observer; it thus contributes to the red wing of the line absorption. As a result, the granule photocenter seen in the blue wing is displaced towards the pole as compared to the granule seen in the continuum (notice that the observed images are due to the photospheric light which is not ab-

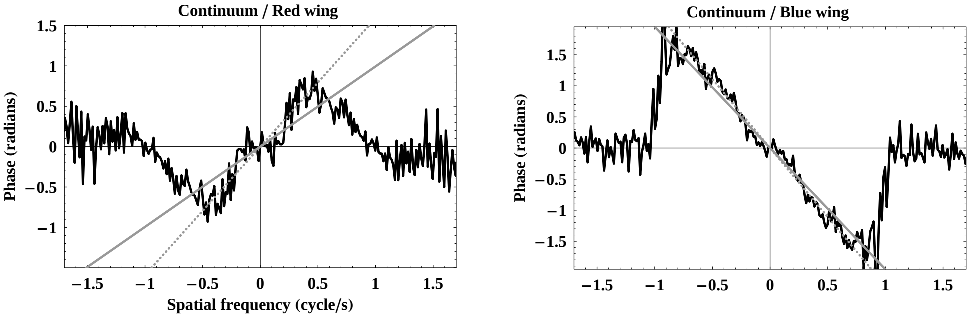

Fig. 3. Unexpected opposite phases in the two wings of the 557.6 nm line. Right figure (resp. left figure) : cross-spectrum have been calculated for the north position $\mu = 0.86$ between the continuum and a wavelength in the red (resp. blue) wing for a line depression coefficient of 0.33 (resp. 0.25).

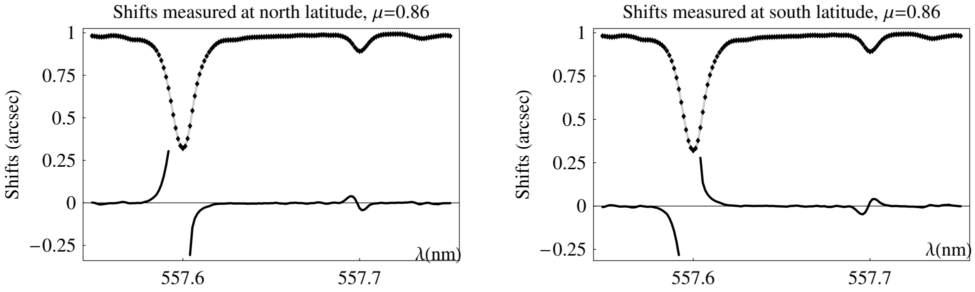

Fig. 4. Shifts measured in the whole CCD λ-domain around 557.6 nm, for $\mu = 0.86$ on the North and the South (resp. right and left figure). Line profile shown in arbitrary units. Measures are completely consistent: the signs of the shifts are opposite for north and south positions. In weak lines, the slope of the cross-spectrum phase is determined quite easily. This is not the case near the core of strong lines.

sorbed...). On the contrary, the granule material moving horizontally towards the disk center comes toward the observer's direction. It thus contributes to the absorption in the blue wing and in the red wing, the photocenter's position is shifted towards the disk center. If these horizontal velocities are not spatially resolved in the spectrograms, they cannot be corrected when we do the pre-processing Doppler-shift compensation in the line.

5.3. Getting the line formation depth

Two different mechanisms may be combined to reproduce our observations. If we do not take into account *C*-shape effects, the perspective effect produces symmetrical shifts at symmetrical wavelengths with respect to line center. The divergent horizontal granular velocity fields produce antisymmetrical shifts. We want to eliminate the displacements caused by velocities effects. In a first attempt, we simply add the shifts obtained in both wings at the same depression level $\delta(\lambda) = (I_C - I_W(\lambda))/I_C$. We expect to observe the perspective effect as an increasing shift going from zero in the continuum (line depression equal to 0), to a maximum at line center (maximum line depression, depending on the line strength).

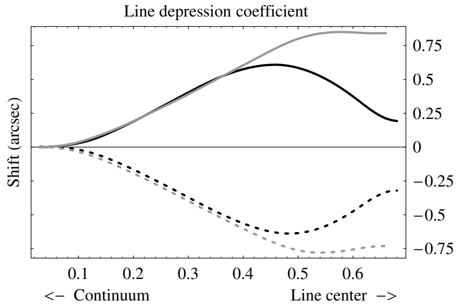

Fig. 5. Results for the Fe I 557.6 nm line. Plain lines : corrected shifts on the North (dark for $\mu = 0.86$ and gray for $\mu = 0.66$). Dotted lines : corrected shifts on the South (dark for $\mu = 0.86$ and gray for $\mu = 0.66$).

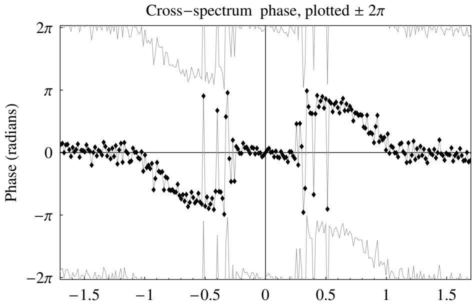

Fig. 6. Phase determination for the north position $\mu = 0.86$, on the 557.6 nm strong line, between the continuum and the line core. It is plotted modulo 2π.

Figure 5 shows the corrected shifts as a function of the line depression level in the Fe I line at 557.6 nm. Their signs are consistent with what we expect for a perspective effect. Near the line center, for observations made at $\mu = 0.66$, we nevertheless observe a non monotonous behavior that is certainly due to residual velocity effects which are not well-corrected by our simple procedure. In particular we do not take into account velocity gradients that give rise the *C*-shaped line profile. The shifts are also significantly larger than the line formation depth computed from the LTE calculation of the line formation, in a 1D quiet solar model (see in Paper [1]).

6. Contrast inversion in the 557.6 nm line

In the previous paragraphs, we described the cross-spectrum technique, and show that it allows small displacements to be detected (see the small line at 557.7nm in Fig.4). We now focus on what happens in the core of the Fe I line at 557.6 nm.

6.1. Effect in the cross-spectrum phase

Figure 6 shows the phase determined between the continuum and a wavelength in the core of the 557.6 nm line (for a line depression coefficient $\delta(\lambda) = 0.39$). Note that we have plotted the phase $\pm 2\pi$ on the same graph, which allows a visual unwrapping of the phase. After this unwrapping, we observe a stepwise monotonous behavior of the phase in the spatial frequency range between 0.3 and 0.5 arcsec^{-1} (resp. -0.3 and -0.5 arcsec^{-1}), with a jump of $+\pi$ (resp. $-\pi$) at a spatial frequency around 0.4 arcsec^{-1} (resp. -0.4 arcsec^{-1}). This jump can be due to a contrast inversion of the fine-scale granular structures between the deep layers of the photosphere and the upper layers where the line core is formed.

A similar reversal is reported by Janssen & Cauzzi (2006) from high angular resolution images obtained at different wavelengths along the profile of the Fe I line at 709.04 nm. It is also present in numerical simulations of the photospheric convection (Nordlund 1985).

6.2. Effect in the cross-correlation

In order to check this interpretation, we calculate the cross-correlations between the 1D intensity variations existing in the continuum and at different wavelengths along the strong Fe I 557.6 nm line. This function is easier to interpret than the cross-spectrum when differences between structures cannot be reduced to a simple shift.

The result is shown in Fig.7 for two symmetrical positions on the solar disk. The line profile is indicated above in gray-levels. We obtain symmetric figures of cross-correlation

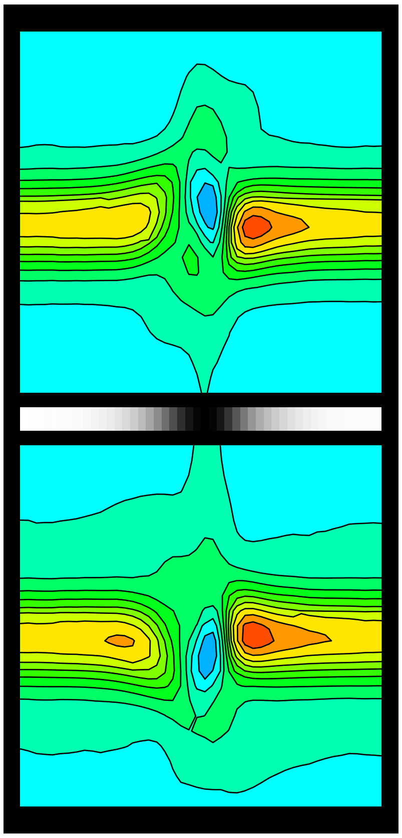

Fig. 7. Cross-correlation functions obtained for symmetrical positions on the Sun, at $\mu = 0.86$ (Top: North; Bottom: South). Abscissa: spectral domain around the Fe I 557.6 nm line (in gray-levels at the figure center). Ordinates: displacements of the photocenter through the line (total range of $\pm 3.4''$). A contrast inversion is detected near the line core.

for opposite positions on the Sun. Close to the continuum, the structures are simply displaced in opposite directions in the two wings of the line. But near the line core, an anti-correlation peak is detected. This is the signature of a contrast inversion between the images of the lower and upper photospheres. From our cross-spectrum analysis, we find that the contrast inversion only affects structures with scales smaller than 2.5", which are typical granular scales.

7. Conclusion.

This paper presents the first use of DSI for solar observations and confirms its feasibility. The DSI technique is not diffraction-limited, and needs no calibration of the atmospheric fluctuations. A 3D investigation of the photospheric solar structures can be done by computing the cross-spectrum between 1D intensity variations observed in the continuum and in spectral lines, and by studying its phase variations.

There are several kinds of difficulties. We need to correct the spectrograms from lines Doppler-shifts due to granular velocities. But the small-scale velocity fields induce uncorrected shifts that are detectable with the DSI technique. That is why we systematically observed opposite shifts in the two wings, instead of measuring shifts caused only by a perspective effect, which would be maximal at line center. The small-scale velocity effect may be eliminated with more refined correction procedures.

For strong lines we detect a contrast inversion between the lower and the upper photosphere. This clearly appears in the phase of the continuum/line core cross-spectrum, as a jump of $\pm\pi$ of the phase. It is detected for spatial scales smaller than 2.5". This anti-correlation peak is also visible in the cross-correlation of the spectrograms, calculated in the line core.

References

Aime, C. 1974, Journal of the Optical Society of America (1917-1983), 64, 1129

Aime, C., Martin, F., Petrov, R., Ricort, G., & Kadiri, S. 1984, A&A, 134, 354

Aime, C., Petrov, R., Martin, F., Ricort, G., & Borgnino, J. 1986, Optical Engineering, 25, 716

Beckers, J. M. & Hege, E. K. 1982, in ASSL Vol. 92: IAU Colloq. 67: Instrumentation for Astronomy with Large Optical Telescopes, ed. C. M. Humphries, 199–206

Grec, C., Aime, C., Faurobert, M., Ricort, G., & Paletou, F. 2007, A&A, in press,

Janssen, K. & Cauzzi, G. 2006, A&A, 450, 365

Nordlund, A. 1985, Sol. Phys., 100, 209